

IMPROVED FLOW PREDICTION IN INTRACRANIAL ANEURYSMS USING DATA ASSIMILATION

F. Schulz¹, C. Roloff¹, D. Stucht², D. Thévenin¹, O. Speck² and G. Janiga¹

¹Department of Fluid Dynamics and Technical Flows, Otto-von-Guericke University Magdeburg,
Magdeburg, Germany
e-mail: {franziska.schulz,christoph.roloff,janiga,thevenin}@ovgu.de

² Department of Biomedical Magnetic Resonance, Otto-von-Guericke University Magdeburg,
Magdeburg, Germany
e-mail: {oliver.speck,daniel.stucht}@ovgu.de

Keywords: CFD, Data Assimilation, Hemodynamics, Intracranial Aneurysm, PC-MRI

Abstract. *Rupture of intracranial aneurysms often leads to irreversible disabilities or even death. The investigation of hemodynamics increases the understanding of cardiovascular diseases, this gain of knowledge can support physicians in outcome prediction and therapy planning. Hemodynamic simulations are restricted by modeling assumptions and uncertain initial conditions, whereas PC-MRI data is affected by measurement noise and artifacts. To overcome the limitations of both techniques, the current study uses a Localization Ensemble Transform Kalman Filter (LETKF) to incorporate uncertain Phase-Contrast MRI data into an ensemble of numerical simulations. The analysis output provides an improved state estimate of the three-dimensional blood flow field. Benchmark measurements are carried out in a silicone phantom model of an idealized aneurysm under user-specific inflow conditions. Validation is ensured with high-resolution Particle Imaging Velocimetry (PIV) obtained from a vertical slice in the center of the same geometry. Results show that even velocity peaks smaller than the PC-MRI resolution can be reconstructed using the employed approach. The root mean square error (RMSE) of the analysis state estimate is reduced by 27 % to 89 % in comparison to interpolation of the PC-MRI data onto the PIV grid resolution.*

1 INTRODUCTION

Computational Fluid Dynamics (CFD) has been frequently used in past studies for the investigation of hemodynamics in intracranial aneurysms. Flow-dependent parameters, such as wall shear stress or the oscillary shear index, are meant to have an influence on the growth and rupture probability of aneurysms [1–3]. However, such simulations require accurate initial and boundary conditions, and depend on the assumptions used in the numerical model [4–6]. Although high temporal and spatial resolution can be reached, uncertainties lead to a limited clinical acceptance of the simulation results [7–9]. Phase-Contrast Magnetic Resonance Imaging (PC-MRI) *in-vivo* measures blood flow by encoding the velocities in the phase of the acquired MR signal [10–12]. In addition to measurement noise and artefacts, the limited temporal and spatial resolution impact clinically-relevant flow features in the measurement data. The present study incorporates uncertain measurement data into numerical simulations by using data assimilation to improve the accuracy and physical correctness of the measured velocity fields. An Ensemble Kalman Filter technique samples the system state and covariance matrices by an ensemble of model states. Thus, the covariance matrices are not calculated directly, but estimated through an ensemble and replaced by the sample covariance. The background uncertainty is estimated and the Ensemble Kalman Filter (EnKF) can be seen as a Monte-Carlo approximation of the original Kalman Filter [13].

Several attempts have been made to improve the accuracy of intracranial velocity fields acquired from PC-MRI data. Whereas de-noising techniques, as well as divergence-free filtering approaches, improve the physical correctness of the velocity field, spatial and temporal resolution remains low e.g. [14, 15]. Hence, data assimilation seems to be a promising remedy to improve resolution while keeping constraints, such as incompressibility and conservation laws. Variational data assimilation approaches in intracranial aneurysms have been applied by D’Elia et al. [16–18] and Funke et al. [19]. As an alternative to the Ensemble Kalman Filters they minimize the error between observations of a reference flow and a numerical estimation in terms of a cost function. The need for linear and adjoint models increases computational complexity by a factor of 50 to 100 in comparison to one simple model simulation. As a consequence, most numerical studies on variational data assimilation in intracranial aneurysms currently address steady-state flow and/or 2D geometries. Funke et al. [19] investigates transient 3D flow fields, but to keep computational costs in an acceptable range, spatial resolution is decreased. Although promising results have been achieved for other fluid dynamical applications e.g. [20, 21], little attention has been paid to the sequential Kalman Filters in intracranial aneurysm modeling. Bakhshinejad et al. implemented an Extended Kalman Filter for pulsatile cardiac flow [22]. Nevertheless, the lack of localization requires a large amount of ensemble members to ensure filter convergence. The resulting high computational costs illustrate the need for a sequential data assimilation technique that can gain convergence with a limited amount of ensemble simulations.

Although the current study deals with steady-state 3D flow, this is the first approach using a Localization Ensemble Transform Kalman Filter to assimilate CFD and PC-MRI data for improved flow prediction in intracranial aneurysm. The study comes along with a systematic analysis of parameters inside the algorithm. Additional uniqueness is ensured with a high quality PIV measurement of the same geometry which enables proper quantitative validation of the assimilation step.

2 MATERIAL and METHODS

Underlying CFD and measurement data for the assimilation step are obtained from the same silicon phantom model of an idealized intracranial aneurysm (figure 1a). Afferent and efferent vessels have a diameter of 4 mm. The phantom model, consisting of two-component silicon (Wacker RT 601, Burghausen, Germany), is well suited because it allows blood flow measurements with the MR device, as well as optical based PIV measurements. A blood substitute, which was required to match both the fluid-dynamical properties of real blood as well as the refractive index of the silicone block ($=1.4122$ at 22°C) for optimal optical conditions within the validation PIV measurements, was formulated.

2.1 Experimental Set-Up

The flow data was acquired on a 7 Tesla whole-body MRI system (Siemens Healthineers, Forchheim, Germany) in a 32-channel head coil (Nova Medical, Wilmington, MA) using 4D phase-contrast magnetic resonance imaging (PC-MRI). Hereby, the acquisition sequence is based on a rf-spoiled gradient echo with quantitative flow encoding in all three spatial dimensions [23, 24]. A micro-gear pump (HNP Mikrosysteme, Schwerin, Germany), placed in the control room of the MRI scanner, delivered a constant flow rate of $Q=227$ mL/min throughout the measurements (figure 1b). This relatively low flow rate was chosen to ensure laminar flow inside the aneurysm which was needed for accurate validation of the data assimilation parameters. A total scan time of approx. 9 minutes achieves a resolution of $0.57 \times 0.57 \times 0.57$ mm in the resulting phase difference images. The same measurement but without activated pump and thus without flow inside the aneurysm-phantom was acquired for reference. The reference data was subtracted from the flow data to obtain purely flow related phase differences. As the flow information is encoded in the phase of the complex MR-Signal, a velocity encode parameter (v_{enc}) is necessary to specify the highest velocity, encoded in one complete phase. For the acquired data, this parameter was set to 0.6 m/s. As a consequence, the signal-to-noise SNR of the acquired images was calculated using the mean of the signal inside the aneurysm and the signal density of the background noise and was found to be $\text{SNR} \approx 55$. The data was post processed using MeVisLab 2.3.1 and the automated tool described in [25]. This includes noise masking, antialiasing and conversion to the format of the commercial software package EnSight (ANSYS Inc., Canonsburg, PA, USA).

2.2 Numerical Background

The ensemble boundary conditions for the CFD simulations are obtained from the MRI blood flow measurements with a specific mean (228 ml/min) and variance (10 ml/min). A structured hexahedral mesh is created using ANSYS IcemCFD (ANSYS Inc., Canonsburg, PA, USA) resulting in approx. 171.000 cells. Ensemble simulations are carried out using the open source software OpenFOAM 5.0 (OpenCFD Ltd., Bracknell, UK). Blood is treated as an isothermal, incompressible fluid (1222 kg/m³) and Newtonian behavior with a constant dynamic viscosity (4.03 mPa s) is assumed. The vessel walls are assumed to be rigid and no-slip boundary conditions and a zero pressure outlet are implemented. Convergence was obtained when the scaled residuals of pressure and momentum decreased below a value of 10^{-6} .

2.3 Data Assimilation Algorithm

The Local Ensemble Transform Kalman Filter applied in this paper was originally introduced by Harlim and Hunt [27, 28] in the field of meteorology and combines the localization method

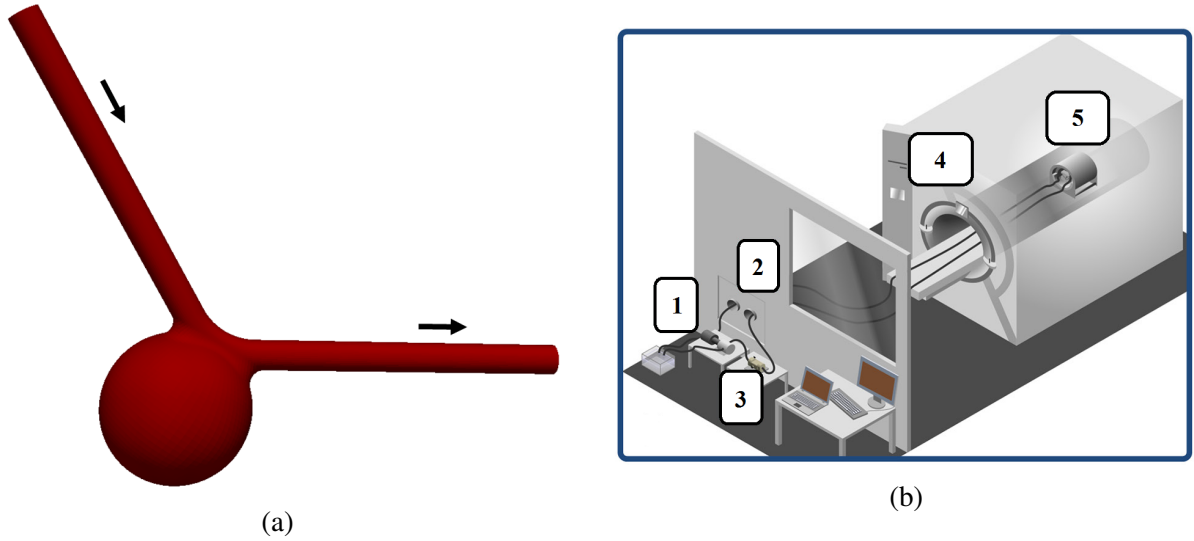


Figure 1: (a) Surface model of the idealized aneurysm used for phantom manufacturing and CFD discretization; (b) MRI setup with the gear pump (1), wave guide through rf-shield (2), flow meter (3), MR-scanner (4) and the 32-channel head coil with the phantom (5) [26].

of the Local Ensemble Kalman Filter (LEKF) of Ott et al. [29] and the Ensemble Transform Kalman Filter (ETKF) of Bishop et al. [30]. The analysis ensemble is formed as a weighted average of the background ensemble mean and the observations. Using background and observation uncertainties, the weights are determined in a way, such that the analysis ensemble mean best fits the given background and observation probability distributions.

With the implementation of the localization, local analyses at each model grid point are obtained. Only observations within a local region surrounding the grid point are accounted for the desired local analysis. The localization scheme enables efficient parallel computation of the analysis model state and limits the number of needed ensemble members. For the current data assimilation experiment a localization radius of 3 mm was chosen.

The following section contains a short summary of the LETKF algorithm. The inputs of the steps below are:

- m -dimensional velocity vectors describing the background ensemble $\{\mathbf{x}^{b(i)} : i = 1, 2, \dots, k\}$ at m grid points for k ensemble members. The ensembles are calculated by k different CFD simulations.
- The s -dimensional observation vector \mathbf{y}^o in the form of a velocity vector obtained from the PC-MRI measurement.
- An observational operator H to map the state variables from the m -dimensional simulation space to the s -dimensional observation space. In the current data assimilation experiment observations, as well as the background ensemble are velocity values. Therefore, the current observation operator H is a spatial binning operator which downsamples the ensemble velocity vectors to the MRI grid resolution.
- An $s \times s$ dimensional observation error covariance matrix \mathbf{R} based on the noise characteristics of the measurement data.

In a first step global transformations are performed with the background ensemble members. Form $\{\mathbf{x}^{b(i)}\}$ into an $m \times k$ dimensional matrix \mathbf{X} and average the columns to get an

m -dimensional vector $\bar{\mathbf{x}}^b$. Subtract this vector from each column of \mathbf{X} to get \mathbf{X}^b .

$$\begin{aligned}\bar{\mathbf{x}}^b &= k^{-1} \sum_{i=1}^k \mathbf{X}^{(i)} \\ \mathbf{X}^{b(i)} &= \mathbf{X}^{(i)} - \bar{\mathbf{x}}^b\end{aligned}\quad (1)$$

By applying the spatial binning observational operator H to each column of \mathbf{X} , the state vector in the model space is transferred to the observational space, followed by a repetition of the previous transformations (equation (1)) with the resulting matrix.

$$\begin{aligned}\mathbf{Y} &= H_l(\mathbf{X}) \\ \bar{\mathbf{y}}^b &= k^{-1} \sum_{i=1}^k \mathbf{Y}^{(i)} \\ \mathbf{Y}^{b(i)} &= \mathbf{Y}^{(i)} - \bar{\mathbf{y}}^b\end{aligned}\quad (2)$$

From this point on local calculations at each model grid point j can be performed, which results in faster convergence of the algorithm due to parallel computations. For each j observations are chosen to be used in the local analysis of a certain grid point. The analysis error covariance matrix $\tilde{\mathbf{P}}^a(j)$ is calculated and used to compute the weight vector $\mathbf{w}^a(j)$.

$$\begin{aligned}\tilde{\mathbf{P}}^a(j) &= \left[(k-1)\mathbf{I}/(1+r) + \left[\mathbf{Y}^b(j) \right]^T \mathbf{R}^{-1}(j) \mathbf{Y}^b(j) \right]^{-1} \\ \mathbf{w}^a(j) &= \tilde{\mathbf{P}}^a(j) \left\{ \left[\mathbf{Y}^b(j) \right]^T \mathbf{R}^{-1}(j) \left[\mathbf{y}^o(j) - H(\bar{\mathbf{x}}^b)(j) \right] \right\}\end{aligned}\quad (3)$$

The desired amount of multiplicative covariance inflation $r = 1.05$ is added to increase the background error. This avoids underestimating the background uncertainty with a small ensemble size.

$$\begin{aligned}\mathbf{W}^a(j) &= [(k-1)\tilde{\mathbf{P}}^a(j)]^{1/2} \\ \mathbf{W}(j) &= \mathbf{W}^a(j) + \mathbf{w}^a(j)\end{aligned}\quad (4)$$

With the weight vector and perturbations, the analysis mean state can be calculated. In the current study it provides an improved state estimate for the velocity field inside the idealized aneurysm geometry. In addition to that, the analysis ensemble members are formatted, which can be used as initial conditions for ensemble simulations in the subsequent step of a transient data assimilation experiment.

$$\begin{aligned}\bar{\mathbf{x}}_l^a(j) &= \bar{\mathbf{x}}_l^b(j) + \mathbf{X}_l^b(j) \mathbf{w}^a(j) \\ \{ \mathbf{x}_l^{a(i)}(j) \} &= \mathbf{X}_n^b(j) \mathbf{X}_l^b(j) \mathbf{W}(j) + \bar{\mathbf{x}}_l^b(j)\end{aligned}\quad (5)$$

2.4 Validation

The generation of a quantitative gold standard is one of the main challenges in the formulation of a suitable data assimilation experiment. High-resolution stereoscopic PIV measurement [26] obtained from a vertical slice in the center of the idealized aneurysm geometry provide a unique possibility for validation. The resulting PIV based velocity fields are sufficiently

accurate to validate the data assimilation procedure. The Root-Mean Square Error (RMSE) between PIV and MRI or analysis, respectively is calculated. To further validate the calculated analysis with respect to physical accuracy, the divergence of the velocity field is calculated. The incompressible flow field inside the aneurysm should fulfill $\text{div}(\vec{v}) = 0$.

To enable reasonable comparisons between the different modalities, the resulting data were registered with the implementation of an Iterative Closest Point (ICP) algorithm. Difficulties in the registration process arise due to geometric distortions in the PC-MRI data. These artefacts increase with the distance to the measurement center, which was chosen to be in the center of the aneurysm sack. For registration purposes, the distorted parts of afferent and efferent vessels are cut, which results in an improved registration of the volume of interest.

3 RESULTS

3.1 PC-MRI data

Figure 3a presents the flow field as well as divergence distribution at different slices acquired from the PC-MRI data. Due to the chosen small flow rate ($Q=227$ mL/min) laminar flow is ensured inside the aneurysm. The velocity fields suffer from acquisition noise and low spatial resolution, both make an accurate definition of the geometric boundaries difficult. In a laminar, incompressible flow field, the divergence should be zero. Data acquired by Phase-Contrast MRI measurements does not automatically fulfill this constraint. Divergence calculated at different slices in the aneurysm geometry highly differs from $\text{div}(\vec{v}) = 0$.

3.2 Data Assimilation

To ensure that the number of ensembles used to calculate the analysis is statistically representative, the RMSE is calculated in dependency of different amounts of ensemble members used in the data assimilation experiment. To suppress the influence of outliers at the geometry edges, different subvolumina are defined in which the RMSE values are compared (figure 2a). Outliers occur due to geometric misfits between MRI, CFD and PIV data, mainly caused by acquisition based distortions of the MRI data. For the current assimilation experiment an ensemble of 10 is chosen to be statistically representative.

Figure 3b represents the velocity fields and divergence of the analysis, the outcome of the data assimilation step. A qualitative comparison between the calculated analysis and the MRI based data reveals a reduction of noise and improvement of image resolution. The latter was achieved by using the CFD grid resolution in the data assimilation algorithm to calculate the analysis. The Navier-Stokes equations as the basis for the ensemble simulations fulfill conservation laws, which results in physically accurate calculated analyses. Divergence in the velocity fields was significantly reduced after the assimilation step.

Figure 4 compares the MRI data and analysis with a vertical slice in the center of the idealized aneurysm. MRI data and analysis are interpolated onto the PIV grid for the calculation of the RMSE in the predefined subvolumina. The small velocity peak at the transition from the aneurysm sack to the efferent vessel completely vanishes in the PC-MRI data. Although, the velocity values are still underestimated by the calculated analysis, the assimilation step was able to reconstruct the flow characteristics at the outlet more accurately. The qualitative investigation is supported by the calculation of the RMSE in all three subvolumina. In two cases the RMSE is significantly reduced by 38 % and 89 %, respectively, whereas for subvolume 2 the RMSE only decreases by 27 %.

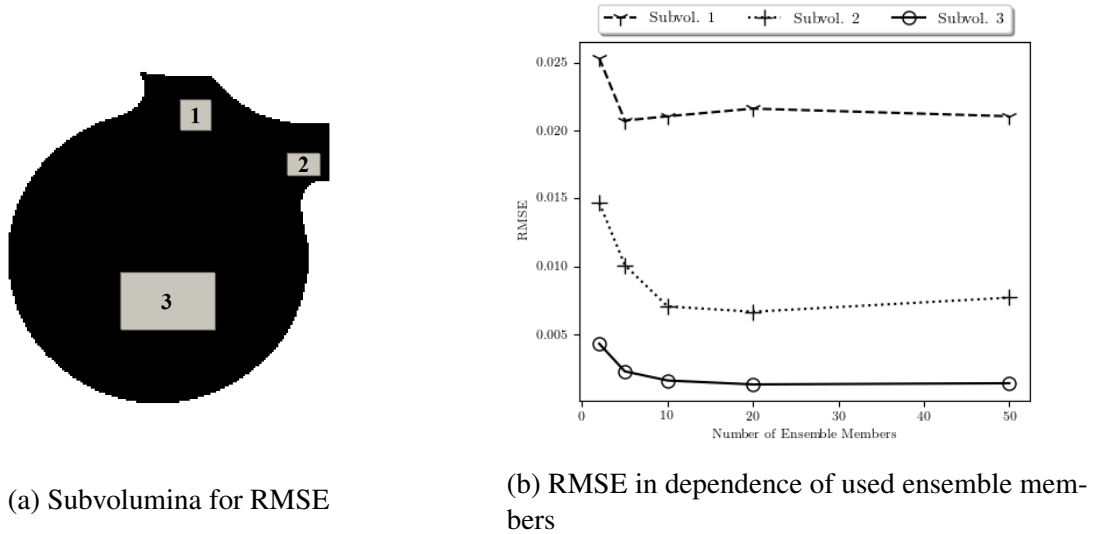


Figure 2: The RMSE in different areas of the aneurysm (a) is calculated in dependency of the number of used ensemble members in the data assimilation algorithm. For the systematic variation of ensemble members, the entries of the observation error covariance matrix are increased to better depict the influence of ensemble simulations

4 DISCUSSION

Flow investigation using Phase-Contrast MRI results in low resolution, noisy images. Optical-based stereoscopic PIV measurements provide high-resolution velocity fields, but can not be used for *in-vivo* applications. The current study uses PIV as a validation criteria for the introduced data assimilation algorithm. An Ensemble Transform Kalman Filter improves the flow prediction in the geometry of an idealized intracranial aneurysm. Although, measured and assimilated flow fields qualitatively predict similar flow characteristics, acquisition noise and artifacts disturb the MRI based velocity fields. Resulting flow fields are not divergence-free, which reduces the physical correctness of the measured data. With the use of the assimilation algorithm conservation laws are introduced into the measurement data, which moves the divergence field closer to zero. By increasing the resolution of the velocity in the analysis, small velocity peaks can be reconstructed that are low-pass filtered in the original measurement data.

In addition to the improvement of physical correctness, the assimilation step moves the velocity field closer to the generated ground truth. The RMSE for the pre-defined subvolumina is reduced by the data assimilation step. Nevertheless, MRI as well as analysis based velocity fields seem to underestimate the general velocity values in comparison to the PIV data. This phenomena also occurs in areas with a uniform velocity distribution, hence downsampling by velocity averaging can not play a major role. These findings lead to the assumption, that it is not only stochastic errors resulting in measurement noise that play a role in the PC-MRI acquisition sequence, rather that systematic deviations also have an influence. Investigations in previous studies, in which PC-MRI data generally underestimates the velocity values, support this fact [26]. Possible factors could be a distortion of the images caused by gradient inhomogeneities in the acquisition sequence. To further reduce the RMSE in the assimilated velocity fields a correct quantification of the systematic error sources is essential, this can be incorporated into the data assimilation algorithm. In a next step, the described data assimi-

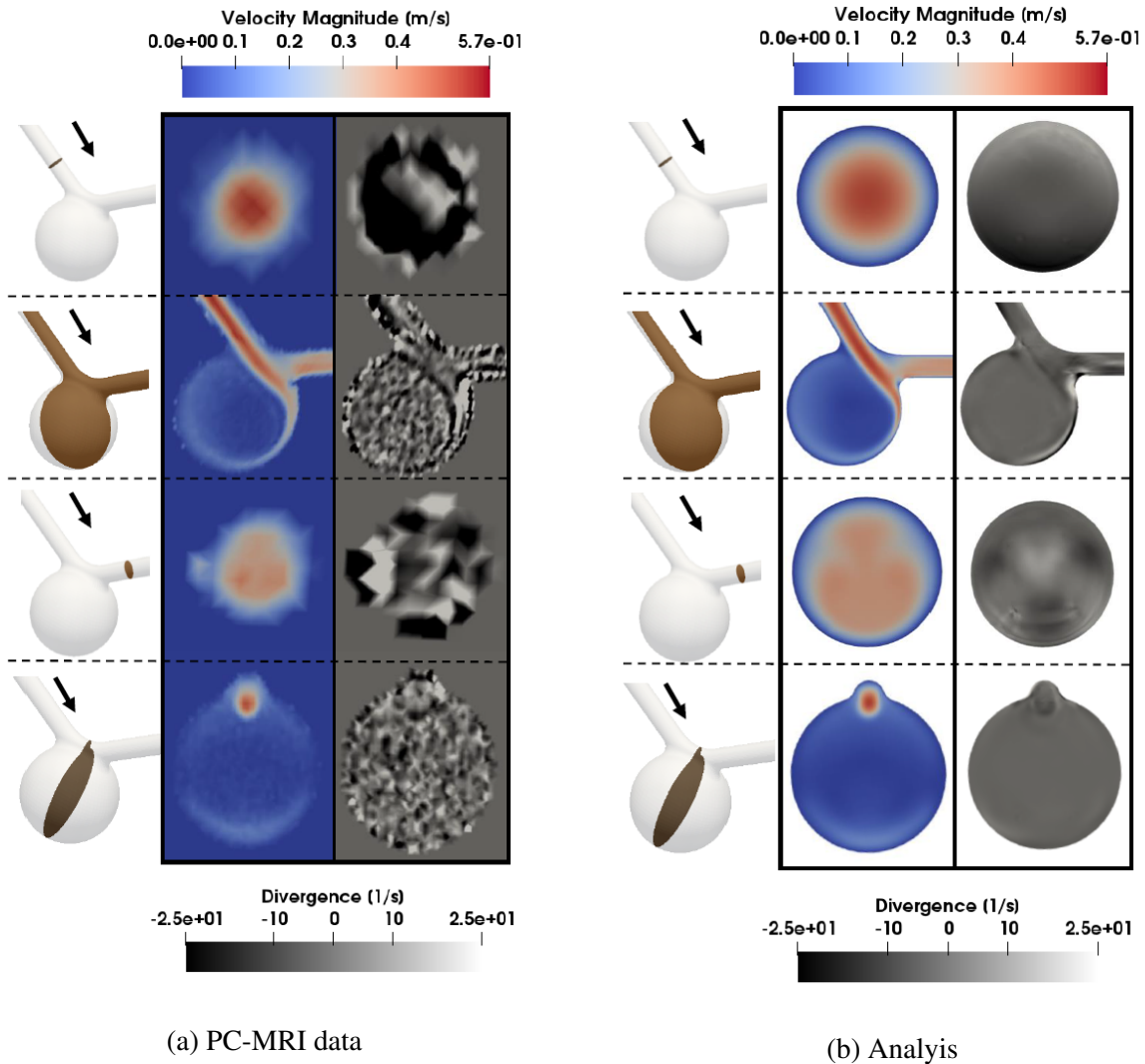


Figure 3: Velocity magnitude and divergence for PC-MRI data (a) and analysis (b) at different cut planes through the underlying geometry.

tion approach is applied to a 3D pulsatile cardiac cycle. Here, specific focus will be paid to the amount of ensemble members needed, which can hopefully be reduced in comparison to [22] with the introduced localization procedure. For patient-specific considerations one of the main difficulties is the accurate definition of geometric boundaries, which will also be a main component in further studies. Incorporating uncertain boundaries of the geometry into the assimilation algorithm could make it suitable for the clinical routine. Further ideas include the projection onto a divergence-free subspace previous to the assimilation step or direct assimilation of phase-difference data by mapping the simulated variables onto the observation space by an inverse observation operator.

5 CONCLUSION

The current study assimilates the flow field in an idealized aneurysm by combining data from numerical simulations together with measured PC-MRI velocity fields. The introduction of PIV measurements originating from the same geometry ensures proper quantitative validation. For

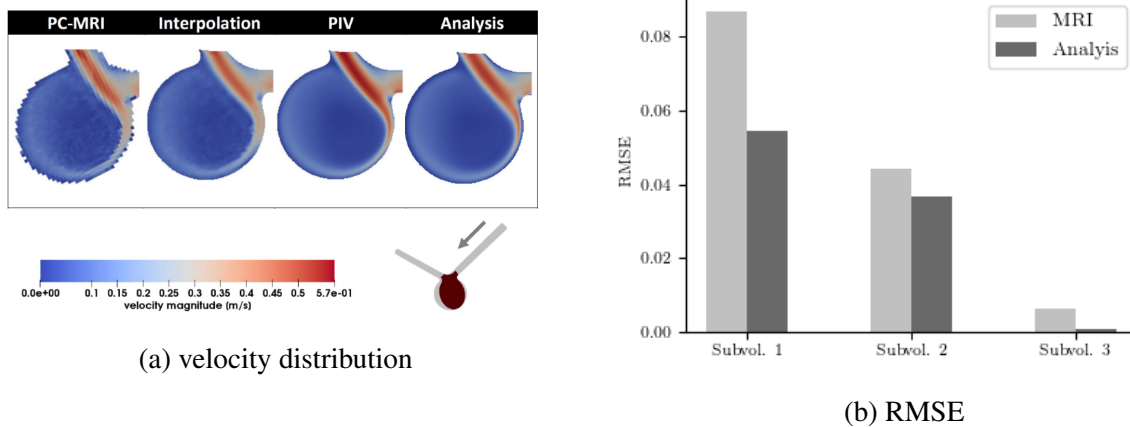


Figure 4: (a) Qualitative comparison of the velocity distribution between all three modalities in PIV grid resolution; (b) RMSE calculation for measured MRI data and calculated analysis in the predefined subvolumina.

the first time the LETKF was used for hemodynamic investigations, which enables the calculation of local analyses. The data assimilation algorithm successfully calculates a high resolution divergence-free velocity field inside the aneurysm geometry. It was able to reconstruct small velocity peaks that have been filtered out by the MRI measurement and reduced the RMSE of the analysis state estimate in comparison to the PC-MRI data.

REFERENCES

- [1] J. R. Cebal, M. Vazquez, D. M. Sforza, G. Houzeaux, S. Tateshima, E. Scrivano, C. Bleise, P. Lylyk, and C. M. Putman, “Analysis of hemodynamics and wall mechanics at sites of cerebral aneurysm rupture,” *Journal of neurointerventional surgery*, vol. 7, no. 7, pp. 530–536, 2015.
- [2] G. Janiga, P. Berg, S. Sugiyama, K. Kono, and D. A. Steinman, “The Computational Fluid Dynamics Rupture Challenge 2013—Phase I: prediction of rupture status in intracranial aneurysms,” *American Journal of Neuroradiology*, vol. 36, no. 3, pp. 530–536, 2015.
- [3] J. Liu, J. Xiang, Y. Zhang, Y. Wang, H. Li, H. Meng, and X. Yang, “Morphologic and hemodynamic analysis of paraclinoid aneurysms: ruptured versus unruptured,” *Journal of neurointerventional surgery*, vol. 6, no. 9, pp. 658–663, 2014.
- [4] I. G. H. Jansen, J. J. Schneiders, W. V. Potters, P. van Ooij, R. van den Berg, E. van Bavel, H. A. Marquering, and C. B. L. M. Majoie, “Generalized versus patient-specific inflow boundary conditions in computational fluid dynamics simulations of cerebral aneurysmal hemodynamics,” *AJNR. American journal of neuroradiology*, vol. 35, no. 8, pp. 1543–1548, 2014.
- [5] C. Karmonik, C. Yen, O. Diaz, R. Klucznik, R. G. Grossman, and G. Benndorf, “Temporal variations of wall shear stress parameters in intracranial aneurysms—importance of patient-specific inflow waveforms for CFD calculations,” *Acta neurochirurgica*, vol. 152, no. 8, pp. 1391–8; discussion 1398, 2010.

- [6] J. Jiang and C. Strother, “Computational fluid dynamics simulations of intracranial aneurysms at varying heart rates: a patient-specific study,” *Journal of biomechanical engineering*, vol. 131, no. 9, p. 091001, 2009.
- [7] J. R. Cebral and H. Meng, “Counterpoint: Realizing the Clinical Utility of Computational Fluid Dynamics—Closing the Gap,” *American Journal of Neuroradiology*, vol. 33, no. 3, p. 396, 2012.
- [8] D. F. Kallmes, “Point: CFD—computational fluid dynamics or confounding factor dissemination,” *AJNR. American journal of neuroradiology*, vol. 33, no. 3, pp. 395–396, 2012.
- [9] C. M. Strother and J. Jiang, “Intracranial Aneurysms, Cancer, X-Rays, and Computational Fluid Dynamics,” *American Journal of Neuroradiology*, vol. 33, no. 6, p. 991, 2012.
- [10] M. Markl, A. Frydrychowicz, S. Kozerke, M. Hope, and O. Wieben, “4D flow MRI,” *Journal of Magnetic Resonance Imaging*, vol. 36, no. 5, pp. 1015–1036, 2012.
- [11] J. Lotz, C. Meier, A. Leppert, and M. Galanski, “Cardiovascular flow measurement with phase-contrast MR imaging: basic facts and implementation,” *Radiographics : a review publication of the Radiological Society of North America, Inc*, vol. 22, no. 3, pp. 651–671, 2002.
- [12] N. Pelc, R. Herfkens, A. Shimakawa, *et al.*, “Phase Contrast Cine Magnetic Resonance Imaging,” *Magnetic resonance quarterly*, vol. 7, 1991.
- [13] G. Evensen, *Data Assimilation - The Ensemble Kalman Filter*. Springer International Publishing, 2nd ed., 2009.
- [14] J. Busch, D. Giese, L. Wissmann, and S. Kozerk, “Reconstruction of divergence-free velocity fields from cine 3d phase-contrast flow measurements,” *Journal of Magnetic Resonance in Medicine*, vol. 69, pp. 200–210.
- [15] M. F. Sereno, B. Köhler, and B. Preim, “Comparison of divergence-free filters for cardiac 4d pc-mri data,” in *Bildverarbeitung für die Medizin 2018*, pp. 139–144, Springer Berlin Heidelberg, 2018.
- [16] M. D’Elia, L. Mirabella, T. Passerini, M. Peregor, M. Piccinelli, C. Vergara, and A. Veneziani, “Applications of Variational Data Assimilation in Computational Hemodynamics.” 2011.
- [17] M. D’Elia, M. Perego, and A. Veneziani, “A Variational Data Assimilation Procedure for the Incompressible Navier-Stokes Equations in Hemodynamics,” *Journal of Scientific Computing*, vol. 52, no. 2, pp. 340–359, 2012.
- [18] M. D’Elia and A. Veneziani, “Uncertainty quantification for data assimilation in a steady incompressible Navier-Stokes problem,” *ESAIM: Mathematical Modelling and Numerical Analysis*, vol. 47, no. 4, pp. 1037–1057, 2013.
- [19] S. W. Funke, M. Nordaas, Ø. Evju, M. S. Alnæs, and K. A. Mardal, “Variational data assimilation for transient blood flow simulations.”

- [20] X. Gao, Y. Wang, N. Overton, M. Zupanski, and X. Tu, “Data-assimilated computational fluid dynamics modeling of convection-diffusion-reaction problems,” *Journal of Computational Science*, vol. 21, pp. 38–59, 2017.
- [21] M. C. Rochoux, B. Cuenot, S. Ricci, A. Trouv, B. Delmotte, S. Massart, R. Paoli, and R. Paugam, “Data assimilation applied to combustion,” *Comptes Rendus Mecanique*, vol. 341, no. 1, pp. 266 – 276, 2013. Combustion, spray and flow dynamics for aerospace propulsion.
- [22] A. Bakhshinejad, V. L. Rayz, and R. M. D’Souza, “Reconstructing Blood Velocity Profiles from Noisy 4D-PCMR Data using Ensemble Kalman Filtering,” in *Biomedical Engineering Society (BMES) - Annual Meeting, Minneapolis, Minnesota*, 2016.
- [23] M. Markl, F. Chan, M. Alley, K. Wedding, M. Draney, C. Elkins, D. Parker, R. Wicker, C. A. Taylor, and R. J. Herfkens, “Time-resolved three-dimensional phase-contrast MRI,” *Journal of Magnetic Resonance Imaging*, vol. 17, no. 4, pp. 499–506, 2003.
- [24] M. Markl, A. Harloff, T. Bley, M. Zaitsev, B. Jung, E. Weigang, M. Langer, J. Hennig, and A. Frydrychowicz, “Time-resolved 3D MR velocity mapping at 3T: Improved navigator-gated assessment of vascular anatomy and blood flow.,” *Journal of Magnetic Resonance Imaging*, vol. 25, no. 4, pp. 824–831, 2007.
- [25] J. Bock, B. Kreher, J. Hennig, and M. Markl, “Optimized pre-processing of time-resolved 2D and 3D phase contrast MRI data.,” in *Proceedings of the 15th Annual Meeting of ISMRM, Berlin, Germany*, , p. 3135, 2007.
- [26] C. Roloff, D. Stucht, O. Beuing, and P. Berg, “Comparison of intracranial aneurysm flow quantification techniques: standard PIV vs stereoscopic PIV vs tomographic PIV vs phase-contrast MRI vs CFD,” *Journal of neurointerventional surgery*, July 2018.
- [27] B. R. Hunt, E. J. Kostelich, and I. Szunyogh, “Efficient data assimilation for spatiotemporal chaos: A local ensemble transform kalman filter,” *Physica D: Nonlinear Phenomena*, vol. 230, no. 1, pp. 112 – 126, 2007. Data Assimilation.
- [28] J. Harlim and B. R. Hunt, “Four-dimensional local ensemble transform Kalman filter: numerical experiments with a global circulation model,” *Tellus A: Dynamic Meteorology and Oceanography*, vol. 59, no. 5, pp. 731–748, 2007.
- [29] E. Ott, B. R. Hunt, I. Szunyogh, A. V. Zimin, E. J. Kostelich, M. Corazza, E. Kalnay, D. J. Patil, and J. A. Yorke, “A local ensemble Kalman filter for atmospheric data assimilation,” *Tellus A: Dynamic Meteorology and Oceanography*, vol. 56, no. 5, pp. 415–428, 2004.
- [30] C. H. Bishop, B. J. Etherton, and S. J. Majumdar, “Adaptive Sampling with the Ensemble Transform Kalman Filter. Part I: Theoretical Aspects,” *Monthly Weather Review*, vol. 129, no. 3, pp. 420–436, 2001.